Early plate tectonics versus single-plate tectonics on Mars: Evidence from magnetic field history and crust evolution

D. Breuer and T. Spohn

Institut für Planetologie, Universität Münster, Münster, Germany

Received 30 October 2002; revised 11 February 2003; accepted 11 March 2003; published 12 July 2003.

[1] The consequences of an early epoch of plate tectonics on Mars followed by single-plate tectonics with stagnant lid mantle convection on both crust production and magnetic field generation have been studied with parameterized mantle convection models. Thermal history models with parameterized mantle convection, not being dynamo models, can provide necessary, but not sufficient, conditions for dynamo action. It is difficult to find early plate tectonics models that can reasonably explain crust formation, as is required by geological and geophysical observations, and allow an early magnetic field that is widely accepted as the cause for the observed magnetic anomalies. Dating of crust provinces and topography and gravity data suggest a crust production rate monotonically declining through the Noachian and Hesperian and a present-day crust thickness of more than 50 km. Plate tectonics cools the mantle and core efficiently, and the core may easily generate an early magnetic field. Given a sufficiently weak mantle rheology, plate tectonics can explain a field even if the core is not initially superheated with respect to the mantle. Because the crust production rate is proportional to temperature, however, an early efficient cooling will frustrate later crust production and therefore cannot explain, for example, the absence of prominent magnetic anomalies in the northern crustal province and the northern volcanic plains in the Early Hesperian. Voluminous crust formation following plate tectonics is possible if plate tectonics heat transfer is inefficient but then the crust growth rate has a late peak (about 2 Ga b.p.), which is not observed. These models also require a substantial initial superheating of the core to allow a dynamo. If one accepts the initial superheating, then, as we will show, a simple thermal evolution model with monotonic cooling of the planet due to stagnant lid mantle convection underneath a single plate throughout the evolution can better reconcile early crust formation and magnetic field generation. *INDEX TERMS:* 6225 Planetology: Solar System Objects: Mars; 5430 Planetology: Solid Surface Planets: Interiors (8147); 5455 Planetology: Solid Surface Planets: Origin and evolution; 5475 Planetology: Solid Surface Planets: Tectonics (8149); 1060 Geochemistry: Planetary geochemistry (5405, 5410, 5704, 5709, 6005, 6008); *KEYWORDS:* Mars, mantle dynamics, mantle differentiation, crust formation, plate tectonics, magnetic field generation

Citation: Breuer, D., and T. Spohn, Early plate tectonics versus single-plate tectonics on Mars: Evidence from magnetic field history and crust evolution, *J. Geophys. Res.*, *108*(E7), 5072, doi:10.1029/2002JE001999, 2003.

1. Introduction

[2] Mars, at present, is a one-plate planet in which heat is generated by radioactive decay and transported to the surface by heat conduction through a single plate lying on top of a convecting mantle. It has a thick crust and does not generate a magnetic field although parts of the crust have been remanently magnetized in the past [*Acuña et al.*, 1999]. Assuming the simplest possible evolution scenario for Mars, the present mode of heat transfer, termed stagnant lid convection [e.g., *Schubert et al.*, 2001], has been operative during the planet's entire evolution. In recent years, however, an early epoch of plate tectonics has been repeatedly proposed for the planet. First, *Sleep* [1994] proposed that the smooth northern lowlands and the Tharsis volcanoes were produced as an ocean floor and an island arc volcanic chain similar to these features on Earth. More recently, the magnetic lineation patterns on parts of the southern highlands detected by Mars Global Surveyor (MGS) have been interpreted to be the result of plate divergence [*Connerney et al.*, 1999], since they are similar to the ocean-ridge-parallel magnetic stripes on Earth. Their broader extent has been suggested to result from a smaller rate of plate divergence.

[3] The differences in heat transfer between stagnant lid convection and plate tectonics are significant. Stagnant lid convection predominantly cools the outer layers of a planet through lithosphere growth while the deep interior is cooled inefficiently. Plate tectonics through lithosphere recycling cools the deep interior efficiently while the lithosphere remains thinner. *Nimmo and Stevenson* [2000], as a further

0148-0227/03/2002JE001999$09.00

argument for an early epoch of plate tectonics, pointed out that the efficient transport of heat from the core by plate tectonics would have helped to sustain thermal convection in the core and dynamo action. Plate tectonics, they argued, would have cooled the core at a rate sufficient to maintain a dynamo even if the core was not initially superheated with respect to the mantle. The early plate tectonics model implies that the tectonic style must have changed at some time in the Martian evolution from plate tectonics to stagnant lid convection. The simplest assumption is that the end of plate tectonics coincided with the end of magnetic field generation. It has been proposed on the basis of the surface distribution of the magnetic anomalies that this event predated the formation of the Hellas basin [*Connerny et al.*, 1999], roughly at the end of the Early Noachian [e.g., *Head et al.*, 2001].

[4] The above timing of the magnetization of the crust has been criticized by *Schubert et al.* [2000], who proposed that the magnetic anomalies were formed well after the formation of Hellas. On the basis of the presently available data neither interpretation can be ruled out, but see *Stevenson* [2001]. In this paper we adopt the model of an early dynamo that ceased to operate at the end of the Early Noachian. A model of Martian tectonics and evolution that explains the generation of an early magnetic field must also provide for the differentiation of the planet and the formation and growth of its crust. Crust growth like dynamo action in the core is strongly coupled to the thermal evolution of the planet; both processes depend on the vigor and mode of convection in the mantle. The present thickness of the Martian crust is not very well known. Models of the interior structure of Mars based on the moment of inertia factor and the chemistry of the SNC meteorites suggest a substantial crust between 100 and 200 km thickness [*Sohl and Spohn*, 1997]. The recent MGS gravity and topography data have been used to calculate variations of the crust thickness over the planet and its average value. Assuming Airy isostasy (or a crust density that is everywhere the same) and further assuming that the floor of the Hellas impact basin defines the minimum crust thickness, an average value of 50 km has been obtained [*Zuber et al.*, 2000]. *Turcotte et al.* [2001] also using the MGS data and assuming that Hellas is ideally compensated in Airy isostasy derived an average crust thickness of 90 km.

[5] The time of crust formation has been constrained using isotope data gathered from SNC meteorites (see *Halliday et al.* [2001] for a recent review) and surface morphological data on volcanic extrusions. The SNC meteorite isotope data suggest an early mantle differentiation event about 4.5 Ga ago with crust and core formation in the Early Noachian and insignificant reservoir mixing thereafter. A recent study of the Nd mass balance in Martian meteorites [*Norman*, 2002] proposes a two-stage formation of the Martian crust with 20–30 km crust formed early, possibly simultaneously with core formation, and 45–75 km thereafter from depleted mantle sources. The exact timing of the second stage, however, cannot be constrained with the geochemical data.

[6] While the surface record of the earliest crust formation is no longer visible in the geological data, it is widely accepted that the bulk of the crust formed in the Noachian [*McEwen et al.*, 1999; *Head et al.*, 2001; *Zuber*, 2001] with possibly widespread volcanic and crust building activity in the Hesperian [*Head et al.*, 2002]. (The Noachian ended 3.5 to 3.7 Ga ago [*Hartmann and Neukum*, 2001] and was followed by the Hesperian that ended 2.9 to 3.15 Ga ago to be followed by the Amazonian.) Early Hesperian volcanism flooded the Northern hemisphere to deposit 1–2 km of volcanic plains deposits onto Noachian crust [*Frey et al.*, 2002]. Considering that volcanic extrusions are usually accompanied by volcanic intrusions that tend to be an order of magnitude more voluminous based on values for the Earth [*Greeley and Schneid*, 1991], roughly 10 to 20 km thickness may have been added to the crust as late as the Hesperian. The absence of magnetic anomalies in most of the Northern hemisphere also suggests that the crust there formed after the cessation of the dynamo if the magnetic anomalies are to be explained by the early dynamo model. The recent detection of young lava flows (<100 Ma) suggests that the planet has been volcanically active in the Amazonian up to the recent past [*Hartmann et al.*, 1999].

[7] The challenge for the early plate tectonics model is thus that it needs to generate a substantial crust with plate tectonics operating in the Early Noachian and that it must allow enough crust to be produced in the post-plate tectonics epoch, most likely in the Middle to Late Noachian and in the Early Hesperian. The plate tectonics model provides crust formation in a two-step fashion (see *Condie* [1997] for a discussion of plate tectonics and the Earth's crust and *Schubert et al.* [2001] for a discussion of plate tectonics and mantle convection). Crust formation is most effective at divergent plate boundaries, where rising hot mantle material crosses the solidus near the surface. This pressure-released melting generates basaltic crust on Earth that is continuously recycled at convergent plate boundaries and it is reasonable to assume that plate tectonics did the same on Mars. More silicic crust is produced in a second differentiation step at convergent plate boundaries where basaltic crust is re-melted (together with continental sediments and possibly mantle rock) to form new continental crust on Earth.

[8] Plate tectonics crusts, judging from the Earth, tend to be thin and ephemeral because of their efficient recycling. The present-day oceanic crust on Earth is only about 8 km thick with a mean age of about 60 Ma. The continental crust has an average age of 2 Ga and is about 36 km thick. It may be speculated that the Earth's oceanic crust was thicker in the past when the mantle temperature as well as the crust production rate was higher. Faster spreading and recycling rates might have counterbalanced this to some extent. *McKenzie and Bickle* [1988] have developed a model of mid-ocean ridge crust production for Earth by considering the volume of melt generated in the mantle. This volume depends on the mantle temperature underneath the ridge and the pressure gradient. The model does not consider melt transfer rates, spreading and subduction rates. Applying their model to Mars results in a thicker crust at the same mantle temperature because of the smaller pressure gradient in this planet. For an upper mantle temperature of about 1600 K, consistent with mantle temperatures in our and *Nimmo and Stevenson*'s [2000] plate tectonics models, a crust thickness of 30 km is obtained. The generation of a 100 km thick basaltic crust requires a mantle temperature of about 1900 K. Although a thick crust could thus be produced at Martian mid-ocean ridges, the question must

be posed whether or not this crust can actually be subducted. Since the crust is less dense than the mantle a thick oceanic crust will make subduction more difficult [e.g., *Davies*, 1998] and may frustrate plate tectonics altogether. Identifying the top thermal boundary layer with the plate tectonics lithosphere, we can estimate the permissible crust thickness for a given potential mantle temperature. Our models give a plate tectonics, convection average boundary layer thickness of 25 to 200 km, depending on initial temperature and mantle reference viscosity. Assuming a thermal expansivity of $4 \cdot 10^{-5}$ K^{-1} and a crust density of 2900 kg m^{-3}, the lithosphere is buoyant with respect to the mantle for a crust thickness of about 30 km and a mantle reference viscosity of 10^{20} Pa s and 44 km for a viscosity of 10^{22} Pa s. It should be noted, however, that these values are upper bounds since crust formation is accompanied by the formation of a depleted harzburgite layer with an even lower density than the undepleted lithosphere and mantle [*Oxburgh and Parmentier*, 1977].

[9] There is no direct evidence for any continental crust on Mars. The andesitic crust in the North most likely formed when plate tectonics was long gone. Models of continental crust growth [e.g., *Gurnis and Davies*, 1985; *Reymer and Schubert*, 1987; *Spohn and Breuer*, 1993; *Breuer and Spohn*, 1995] suggest that continental crust growth on Earth leads to an approximate equilibrium between crust growth and recycling after about 1 to 1.5 Ga. In contrast to oceanic crust where a slower plate drift rate (and mantle convection speed) results in a thicker crust, for the continental crust the production rate is proportional to the mantle convection speed which should be smaller on Mars than on Earth because it scales with planet size. In addition, the continental crust growth rate decreases with decreasing length of the subduction zones and therefore decreases with increasing continental crust area. It is thus difficult to see how Martian plate tectonics could build a thicker continental crust than Earth in half to a third of the available time. Thus the plate tectonics crust thickness is smaller or at most marginally consistent with the minimum thickness of about 50 km. Significant crust production postdating the plate tectonics epoch remains to be explained.

[10] In the stagnant lid regime, there is no crust recycling and there is no two-stage differentiation. Instead, melt is formed underneath the lithosphere usually at greater depth than with plate tectonics. Crust growth is limited by the increasing thickness of the lithosphere as the planet cools because melt buoyancy decreases with increasing depth to the source region (the melt is more compressible than the mantle rock). In addition, the permeability of the lithosphere to magma ascent decreases with increasing thickness and pressure. Assuming stagnant lid convection for the entire evolution of Mars a continuous decrease of the average crust production rate in time with most of the crust being produced in the first few hundred million years has been found by *Weizman et al.* [2001] and *Hauck and Phillips* [2002]. Their models show a global melt zone underneath the lithosphere that is present for a significant part of the Martian evolution, in some models even at present. The evolution of the crust production rate is in general compatible with the constraints on the crust evolution on Mars.

[11] Whether or not an early phase of plate tectonics is compatible with the observational constraints on the crustal evolution of Mars will be examined in the present paper. We have calculated thermal evolution models of Mars assuming an early plate tectonics epoch followed by stagnant lid convection. The models include the effects of mantle differentiation by crust formation after the end of the plate tectonics epoch. The results will be compared to those for a model assuming stagnant lid convection throughout the entire evolution of Mars. It will be shown that models assuming an early phase of plate tectonics are more difficult to reconcile with the widely accepted crust formation history than the more simple thermal evolution models with stagnant lid convection during the entire evolution. Stagnant lid models require some early superheating of the core to explain an early magnetic field.

2. Model

[12] For simplicity, we begin by describing the stagnant lid model that we then modify to account for early plate tectonics.

2.1. Stagnant Lid Convection

[13] We extend the model of *Grasset and Parmentier* [1998] by including core cooling and crust formation with redistribution of radioactive elements from the mantle to the crust. We have checked the validity of our parameterization with full 3d numerical convection calculations in a spherical shell with strongly temperature dependent viscosity and with a cooling core.

[14] The silicate mantle of Mars is thought to be peridotitic in composition, similar to the Earth's mantle [e.g., *Basaltic Volcanism Study Project* (*BVSP*), 1981; *Sohl and Spohn*, 1997]. The first liquid that forms upon melting is basaltic. With further melting, the mantle becomes depleted in this component and the melting temperature increases, thereby eventually frustrating crust formation. A simple way to parameterize this effect is by assuming a constant melting temperature and a finite volume of the basalt component. If the mantle were completely depleted of the crust component the crust would have its maximum thickness D_{pot}. This approach has been used by *Turcotte and Huang* [1990], *Spohn* [1991], *Schubert et al.* [1992], and *Breuer and Spohn* [1995]. The crust growth rate is then given by

$$\frac{dD_c}{dt} = \frac{D_{pot} - D_c}{D_m} u\, m_a \frac{V_a}{V_m} \tag{1}$$

where D_c is the thickness of the crust, t is time, D_{pot} is the constant potential crust thickness, D_m is the mantle thickness, u is the mean mantle velocity, m_a is the mean melt content in the asthenosphere, V_a is the volume of the asthenosphere, and V_m is the volume of the mantle. All of these quantities are functions of time accept for D_{pot}. The first term on the right hand side of equation (1) models the decrease of the crust growth rate with mantle depletion in the assumed crust component. Assuming the entire Martian crust to be basaltic, the potential crust thickness D_{pot} is about 250 km. This thickness corresponds to a mass fraction of the crust component in the silicate shell of the

planet of 0.2 and may be an overestimate considering the evidence for more silicic parts of the present crust from the Thermal Emission Spectrometer (TES) on board MGS [*Bandfield et al.*, 2000]. As the parent magma is likely more fractionated, its concentration in the mantle should be smaller than the value for basalt [*BSVP*, 1981]. However, the difference in the potential crust thickness is small and of no consequence for the results of our present calculations. The second term in equation (1) gives the dependence of the crust growth rate on the mean mantle convection speed u and the concentration of the melt in the mantle. The mantle convection speed u is calculated from

$$\mathrm{u} = \mathrm{u}_0 \mathrm{Ra}^{2\beta} \tag{2}$$

where u_0 is a convection speed scale, Ra is the mantle Rayleigh number and β is a constant equal to 0.3 derived from boundary layer theory and experiments [e.g., *Turcotte and Schubert*, 1982]. We have confirmed the values of u_0 and β with our own spherical 3d mantle convection calculations. The Rayleigh number is defined as

$$\mathrm{Ra} = \frac{\alpha \rho_\mathrm{m} g \Delta \mathrm{T} (\mathrm{R_l} - \mathrm{R_c})}{\kappa \eta} \tag{3}$$

where α is the thermal expansion coefficient, g is gravity, ρ_m is the mantle density, ΔT is the temperature difference across the convecting (sub-lithosphere) mantle minus the adiabatic temperature difference, κ is the mantle thermal diffusivity, R_l and R_c is the radius of the convecting mantle and the core, and η is the temperature-dependent viscosity:

$$\eta = \eta_0 \exp\left(\frac{\mathrm{A}}{\mathrm{RT_m}}\right) \tag{4}$$

with η_0 a viscosity constant, A the activation energy for viscous deformation, and R the gas constant. T_m is the absolute potential temperature of the convecting mantle. (The potential temperature is the temperature corrected for the adiabatic temperature increase caused by pressure.) The concentration of melt in the mantle is equal to the product between m_a, the concentration of melt in the asthenosphere, and the ratio between the volumes of the asthenosphere V_a and the mantle V_m. The thickness and extent in depth of the global melt zone has been obtained by intersecting the solidus of the mantle material and the mantle temperature profile. Assuming a linear increase of melt between the solidus and the liquidus, the mean degree of melting in the asthenosphere is given by:

$$\mathrm{m_a} = \frac{1}{\mathrm{V_a}} \int_{\mathrm{V_a}} \frac{\mathrm{T_m} - \mathrm{T_{sol}}}{\mathrm{T_{liq}} - \mathrm{T_{sol}}} \mathrm{dV} \tag{5}$$

with the solidus of peridotite T_{sol} = 1409. + 134.2 P − 6.581 P^2 + 0.1054 P^3, the liquidus T_{liq} = 2035. + 57.46 P − 3.487 P^2 + 0.0769 P^3 [*Takahashi*, 1990] (temperatures are in K and pressure P is in GPa).

[15] To obtain the lithosphere thickness D_l, we solve the equation for lithosphere thickening and specifically calculate the contributions of volcanic heat transfer and heat conduction to the overall heat transfer rate through the lithosphere [e.g., *Breuer et al.*, 1993]:

$$\rho_\mathrm{m} C_\mathrm{m} (\mathrm{T_m} - \mathrm{T_l}) \frac{\mathrm{dD_l}}{\mathrm{dt}} = -\left(\mathrm{q_m} - (\rho_\mathrm{cr} \mathrm{L} + \rho_\mathrm{cr} C_\mathrm{cr} (\mathrm{T_l} - \mathrm{T_0})) \frac{\mathrm{dD_c}}{\mathrm{dt}}\right) + \mathrm{k} \frac{\partial \mathrm{T}}{\partial \mathrm{z}}\bigg|_{\mathrm{z}=1} \tag{6}$$

where ρ_m is the mantle density, C_m is the mantle heat capacity, T_l is the temperature at the base of the lithosphere, q_m is the heat flow from the convecting mantle into the base of the lithosphere, ρ_{cr} is the crust density, L is the latent heat, C_{cr} is the magma heat capacity, T_0 is the surface temperature, k is the mantle thermal conductivity, and $\partial T/\partial z|_{z=1}$ is the temperature gradient at the base of the lithosphere. The rate of lithosphere thickening is proportional to the difference between the heat flow from the mantle into the base of the lithosphere ($q_m - (\rho_{cr} L + \rho_{cr} C_{cr} (T_l - T_0)) dD_c/dt$ and the heat flow from the base of the lithosphere $k\,\partial T/\partial z|_{z=1}$. The heat flow into the base of the lithosphere is equal to the heat flow q_m from the convecting mantle minus the heat transferred per unit area and time through the lithosphere by volcanism ($\rho_{cr} L + \rho_{cr} C_{cr} (T_l - T_0)) dD_c/dt$ which bypasses the lithosphere. In writing equation (6) we have neglected the small adiabatic temperature increase across the lithosphere. *Schubert et al.* [1979], *Spohn and Schubert* [1982], *Schubert and Spohn* [1990], *Spohn* [1991], and *Breuer et al.* [1993] have previously used versions of equation (6) to calculate the evolution of lithosphere thickness. In contrast to this earlier work in which the temperature at the base of the lithosphere was assumed constant at about 1073 K, we use the results of recent work on convection in fluids with strongly temperature dependent viscosity and identify the lithosphere with the stagnant lid. The basal temperature of the stagnant lid is the temperature at which the viscosity in the convecting layer has increased from its value at the temperature of the convecting sub-layer by one order of magnitude. Thus the lithosphere basal temperature depends on the mantle temperature as well as on the rate of change of viscosity with temperature [*Davaille and Jaupart*, 1993; *Grasset and Parmentier*, 1998; *Choblet and Sotin*, 2000]. More formally,

$$\mathrm{T_l} = \mathrm{T_m} - 2.21 \frac{\eta(\mathrm{T_m})}{\mathrm{d}\eta/\mathrm{dT}} = \mathrm{T_m} - 2.21 \frac{\mathrm{R}}{\mathrm{AT_m^2}} \tag{7}$$

[16] The heat transport in the mantle underneath the stagnant lid can be calculated with the equation based on constant viscosity laws. To calculate the thermal evolution, the following energy balance equations for the mantle and the core have been solved:

$$\rho_\mathrm{m} C_\mathrm{m} V_\mathrm{m} \varepsilon_\mathrm{m} \frac{\mathrm{dT_m}}{\mathrm{dt}} = -\mathrm{q_m} A_\mathrm{m} + \mathrm{q_c} A_\mathrm{c} + \mathrm{Q_m} V_\mathrm{m} \tag{8}$$

$$\rho_\mathrm{c} C_\mathrm{c} V_\mathrm{c} \varepsilon_\mathrm{c} \frac{\mathrm{dT_c}}{\mathrm{dt}} = -\mathrm{q_c} A_\mathrm{c} \tag{9}$$

with A_m the surface area of the mantle, A_c the surface area of core, ρ_c the density of the core, C_c the heat capacity of the core, V_c the volume of the core, T_c the mean temperature of the core, q_c the heat flow out of the core, ε_m the ratio between the mantle temperature representative of the internal energy of the mantle and T_m, ε_c the ratio between the core temperature representative of the internal energy of the core and T_c, and Q_m the heat source density in the mantle.

[17] The heat flow from the convecting sub-layer of the mantle is given by

$$q_m = k\frac{T_m - T_l}{\delta_u} \tag{10}$$

with δ_u the thickness of the upper thermal boundary layer:

$$\delta_u = (R_l - R_c)\left(\frac{Ra}{Ra_{crit}}\right)^{\beta} \tag{11}$$

with Ra_{crit} the critical Rayleigh number. The heat source density in the mantle Q_m decreases with time due to the decay of radioactive elements and as a consequence of the irreversible transfer of mantle heat sources to the crust. The decrease with time is given by

$$Q_m = Q_0 \exp(-\lambda t)\left(1 - \Lambda\frac{V_c}{V_m}\right) \tag{12}$$

with Q_0 the initial heat production density in the mantle, λ the mean decay constant of the radioactive elements, Λ the crust over mantle radiogenic element enrichment factor, and V_c the volume of the crust with time. We assume the crust enrichment factor to be constant with a value of 4. Although this is a simplification, our results are similar to those of more detailed models in which the concentration of heat sources in the crust forming melt depends on the melt fraction [e.g., *Hauck and Phillips*, 2002]. Using the approach of *Hauck and Phillips* [2002], the enrichment factor varies between 10 and 2 for degrees of partial melting between 0 and 40%, respectively. The mean melt concentration in our models for most of the time is between of 10 and 20% giving enrichment factors between 5 and 3.5. These values are close enough to our assumed value of 4.

[18] The heat flow q_{cm} out of the core into the mantle is calculated, using a local stability criterion for the core/mantle thermal boundary layer [e.g., *Stevenson et al.*, 1983]

$$q_c = k\frac{\Delta T_{cm}}{\delta_c} \tag{13}$$

with $\Delta T_{cm} = T_c - \varepsilon_{cm} T_m$ the temperature difference across the thermal core-mantle boundary layer (ε_{cm} accounts for the adiabatic temperature increase through the mantle), and δ_c the thickness of the boundary layer

$$\delta_c = \left(\frac{\kappa\eta_c Ra_{crit}}{\alpha\rho_m g_{cm}\Delta T_{cm}}\right)^{\frac{1}{3}} \tag{14}$$

where η_c is the geometrically averaged viscosity in the thermal boundary layer and is given by [*Richter*, 1978]

$$\eta_c = \eta_0 \exp\left(\frac{A}{R(T_{cm} - \Delta T_{cm}/2)}\right) \tag{15}$$

and g_{cm} is the gravity at the core/mantle boundary. The core will be convecting and generate a magnetic field if the heat flow q_c exceeds the conductive heat flow along the core adiabat q_{ad}, which is given by

$$q_{ad} = \frac{k_c \alpha_c g_{cm} T_c}{C_c} \tag{16}$$

with k_c and α_c the thermal conductivity and expansivity of the core, respectively. It is possible that the core freezes and that a chemically driven dynamo generates a magnetic field [*Stevenson et al.*, 1983]. However, it is one of the results of our calculations to be shown below that the core temperature is very likely always to be greater than the core liquidus even for small concentrations of sulfur or other possible light elements. Since an entire liquid core offers the best explanation for the present absence of a magnetic field on Mars [*Schubert and Spohn*, 1990] (the alternative being a completely frozen core), we will not consider core freezing in this paper.

2.2. Early Plate Tectonics

[19] For the early phase of plate tectonics the thermal evolution is calculated using the constant viscosity convection parameterization. This simple parameterization scheme has been noticed to reproduce heat transfer by mantle convection with plate tectonics satisfactorily well [e.g., *Schubert et al.*, 2001]. The model is similar to the preceding stagnant lid model. The only difference is in the top boundary condition: While in the stagnant lid model the temperature is T_l at $z = l$, in the plate tectonics model the boundary condition is $T = T_s$ at $z = 0$.

[20] At time t_{cp} plate tectonics ceases to operate. The transition from plate tectonics to single-plate stagnant lid convection is, basically, an unknown process. There are no known direct observations that may guide our modeling. What is known is that in an isothermal fluid, which is suddenly cooled from above and therefore unstable to thermal convection, the fluid will begin to flow only after a conductive layer of sufficient thickness has formed underneath the cooling surface. If the viscosity is strongly temperature dependent, this layer will consist of a stagnant lid and a thermal boundary layer. The thickness of the thermal boundary layer can be calculated using a boundary layer stability criterion [*Choblet and Sotin*, 2001] and for internally heated convection is given by

$$l_{crit} = \left(\frac{\kappa\eta Ra_{crit}}{\alpha\rho_m g(T_m - T_l)}\right)^{\frac{1}{3}} \tag{17}$$

[21] The temperature drop across the thermal boundary layer is $T_m - T_l$, where T_l is calculated from equation (7) and Ra_{crit} is equal to 450 [*Choblet and Sotin*, 2000]. For the onset of bottom-heated convection, *Solomatov* [1995] gives

the following critical thickness for the entire conductive layer (stagnant lid plus thermal boundary layer)

$$L_{crit} = 2.75\left(\frac{\eta_{cm}\kappa}{\alpha\rho_m g}\right)^{\frac{1}{3}}\left(\frac{R}{AT_m^2}\right)^{\frac{4}{3}}(T_{cm} - T_s) \qquad (18)$$

where η_{cm} is the viscosity at the core/mantle boundary.

[22] Note that in the latter formulation the critical thickness depends on the temperature at the core/mantle boundary and the viscosity there. The surface thermal boundary layer with plate tectonics is significantly thinner than the critical thicknesses given by equations (17) and (18). The thinner boundary layer together with the smaller temperature difference across the boundary layer implies that the heat flow associated with plate tectonics is larger. (The temperature difference is $(T_m - T_l)$ in the case of stagnant lid convection and $(T_m - T_s)$ for plate tectonics.) As a consequence, a simple transition from plate tectonics to stagnant lid convection will be accompanied by a jump in heat flow from the convecting mantle and a discontinuity in the slope of the surface heat flow versus time curve as well as a discontinuity in the evolution of the boundary layer thickness. To avoid these discontinuities, *Nimmo and Stevenson* [2000] have assumed that mantle convection ceases to operate together with plate tectonics and that heat is transferred in the mantle by heat conduction until the heat flow has decreased to the value that can be carried by stagnant lid convection and until the surface boundary layer has reached the necessary thickness given by equation (18).

[23] It seems to us unlikely, however, that after vigorous convection with plate tectonics, convection will stop altogether when the plates stop to subduct although we admit that the mantle flow at infinite Prandtl number has no inertia and could stop at any time. Rather, we believe that convection continues, since the mantle continues to be unstable to convection, underneath the plates that may have become stuck because the crust became to thick to be subducted. It may also be possible that plate tectonics continues for some time underneath a buoyant crust, similar to the model of lithosphere delamination, before the lid becomes entirely stagnant. The viscosity contrast in the convecting mantle is basically infinite in the plate tectonics regime whereas in the stagnant lid regime the contrast is of the order of a factor of 10 [e.g., *Davaille and Jaupart*, 1993; *Grasset and Parmentier*, 1998]. We assume that once plates are no longer subducted, convection will immediately stop where the viscosity is above the factor of 10 threshold, thereby immediately forming a stagnant lid. The heat flow from the mantle will immediately decrease by the factor of $(T_m - T_s)/(T_m - T_l)$. The temperature in the lid, the thickness of the boundary layer underneath the lid, the heat flow through the lid, and the surface heat flow will then adjust in the time following the transition.

[24] Because the transition may be critical for the model, we compare before we proceed the two transition models in their effect on the thermal evolution of the mantle. We modify the model of *Nimmo and Stevenson* [2000] by explicitly solving the time-dependent heat conduction equation to calculate the temperature distribution of the planet during the transitional phase when heat is assumed to be transferred by conduction and by using equation (17) instead of (18) because we believe that the criterion should be independent of the properties of the core/mantle boundary not the least because mantle convection in Mars is mostly heated from within. Following Nimmo and Stevenson, T_m is calculated at

$$z = L_0 + \sqrt{4\kappa(t - t_{cp})} \qquad (19)$$

with L_0 the thickness of the thermal boundary layer at the time of cessation of plate tectonics, t_{cp}. Figure 1a shows two conductive temperature profiles taken at two consecutive times after the cessation of plate tectonics; indicated is also the bottom temperature T_l and the temperature T_m. The critical thickness of the upper thermal boundary layer is reached and stagnant lid convection sets in after 300 Ma. This is a factor of about three shorter than the transition time calculated by *Nimmo and Stevenson* [2000]. The difference of the length of the transitional stage may be caused by the more accurate determination of the temperature profile during conductive cooling for the presented model and by the difference in using equation (17) instead of (18).

[25] Figure 1b shows the evolution of the mantle temperature for the two transition models. The difference between the two models is actually quite small. For an instantaneous transition from plate tectonics to stagnant lid convection, the mantle temperature is a few tens of degrees higher (Figure 1b) than in the *Nimmo and Stevenson* [2000] model and the lithosphere thickness (not shown in Figure 1) is a few tens of kilometers thicker.

2.3. Parameter Values

[26] The thermal evolution models have been calculated assuming that core formation is completed at time t = 0. We further assume the potential mantle and core temperature to both be equal to 2000 K. Thus there is no initial super heating of the core. The heat source density for the present primitive mantle (mantle plus crust) has been estimated from the concentration of incompatible elements in the SNC-meteorites [e.g., *Dreibus and Wänke*, 1985; *Treiman et al.*, 1986]. We used the values of 16 ppb U and the ratios of the concentrations K/U of 10^4 and Th/U of 3 [*Treiman et al.*, 1986]. Using the radioactive decay constants and the rates of heat release of these elements [e.g., *BVSP*, 1981], an initial heat production density of the primitive mantle after core formation of $Q_0 = 1.6 \cdot 10^{-8}$ W/m^3 is obtained. The critical heat flow from the core for dynamo action is uncertain by a factor of about 4 and ranges from 5 to 19 mWm^{-2} [*Nimmo and Stevenson*, 2000]. This range of values has been calculated using values for the thermal conductivity k_c of 43–88 Wm^{-1}K^{-1}, $\alpha_c = 2 \cdot 10^{-5}$ K^{-1}, and $C_c = 840$ Jkg^{-1}K^{-1} and considering their uncertainties.

[27] Mantle rheology parameters and the assumed length in time of the plate tectonics regime are the most important parameters and their values have been varied. An activation energy of about 300 kJ/mole is representative of dry olivine at zero pressure [*Karato and Wu*, 1993], which is most likely the primary mineral of a dry planetary mantle. However, the viscosity increases as a function of depth and a value of A equal 540 kJ/mole is proposed for a Martian mid-mantle pressure of about 12 GPa [*Karato and Wu*,

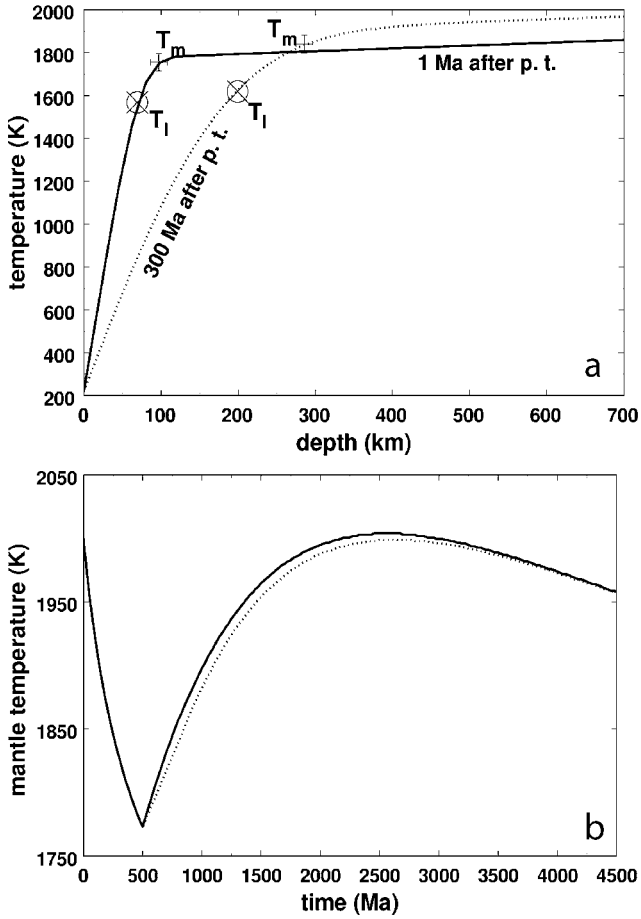

Figure 1. a) Temperature profile in the upper mantle 1 Ma (solid line) and 300 Ma (dotted line) after cessation of plate tectonics. It is assumed that after cessation of plate tectonics the mantle cools by conduction only until stagnant lid convection sets in. Indicated is the position of the cold front (T_m) and the potential bottom temperature of the stagnant lid (T_l, calculated by equation (7)). One million years after cessation of plate tectonics the lower part of the cold front (between T_m and T_l) is much thinner than the calculated critical thickness (equation (17)). After 300 Ma the lower part of the cold front approaches the critical boundary layer thickness, stagnant lid convection can set in. b) Mantle temperature as a function of time for two different transitional stages after cessation of plate tectonics: thermal conduction after cessation of plate tectonics until stagnant lid convection set in (dotted line) and direct onset of stagnant lid convection after cessation of plate tectonics (solid line).

1993]. We have used both values of 300 and 540 kJ/mole. The particular significance of A lies with the fact that it enters equation (7) for T_l. The viscosity constant η_0 has been calculated by assuming that the viscosity η takes values between 10^{20} and 10^{22} Pas for a potential mantle temperature of 1600 K. These values are similar to estimates for the present-day Earth's mantle [e.g., *Peltier*, 1996]. The length of the plate tectonics regime has been varied between 200 and 600 Ma after core formation but is 500 Ma for most models. All other parameter values are given in Table 1.

3. Results

3.1. Early Plate Tectonics Models

[28] In a first step, we present the results for early plate tectonics models and discuss the effects of mantle rheology on the thermal evolution, the growth history of the crust after the plate tectonics epoch, and core convection during the latter epoch as a prerequisite for magnetic field generation. We cast our discussion in terms of the three reference models EPT20, EPT21 and EPT22 with reference viscosities of 10^{20} Pas, 10^{21} Pas and 10^{22} Pas, respectively. We will compare these results in the section following the present one with those obtained for the equivalent stagnant lid models STL20, STL21 and STL22. Note also that we do not include crust formation during plate tectonics in this section, thereby giving post-plate tectonics crust formation the full potential. The consequences of crust growth during plate tectonics will be discussed further below.

[29] As a general result we observe that plate tectonics causes a strong cooling of the planet's interior during its time of operation. Depending on the chosen reference viscosity, the mantle temperature decreases from a common starting value of 2000 K to about 1650–1900 K in the first 500 Ma, the assumed length of the plate tectonics regime (Figure 2). The efficiency at cooling increases with decreasing reference viscosity. After plate tectonics has ceased, mantle temperature increases again for about 2 Ga as a consequence of the comparatively inefficient heat transport of stagnant lid convection. The resulting increase in mantle temperature by about 200 K is largely independent of the reference viscosity. Thereafter, the interior cools slowly due to the decay of the radiogenic heat sources and due to secondary cooling; the present-day mantle temperatures are between 1800 and 2100 K. The stagnant lid grows rapidly (Figure 3) by about 300 to 400 km in the first 500 to 1000 Ma, simultaneously with the temperature increase in the mantle. The present-day thickness of the lid is between 350 and 500 km.

Table 1. Definition and Values of Parameters

Parameter	Notation	Value	Unit
Radius of planet	R_p	3400×10^3	m
Radius of core	R_c	1700×10^3	m
Surface gravity acceleration	g	3.7	m/s^2
Surface temperature	T_0	220	K
Core density	ρ_c	7200	kg/m^3
Core heat capacity	C_c	840	J/(kg K)
Average/upper core temperature	ε_c	1.1	
Mantle density	ρ_m	3500	kg/m^3
Mantle heat capacity	C_m	1142	J/(kg K)
Mantle thermal conductivity	k	4	W/(m K)
Mantle thermal expansivity	α	2×10^{-5}	K^{-1}
Mantle thermal diffusivity	κ	10^{-6}	m^2/s
Average/upper mantle temperature	ε_m	1.15	
Convection speed scale	u_0	10^{-12}	m/s
Gas constant	R	8.3144	J/(mole K)
Crust density	ρ_{cr}	2900	kg/m^3
Magma heat capacity	C_{cr}	1000	J/(kg K)
Latent heat of melting	L	$6 \cdot 10^5$	J/kg
Crust over mantle radiogenic element enrichment factor	Λ	5	
Potential crust thickness	D_{pot}	$250 \cdot 10^3$	m

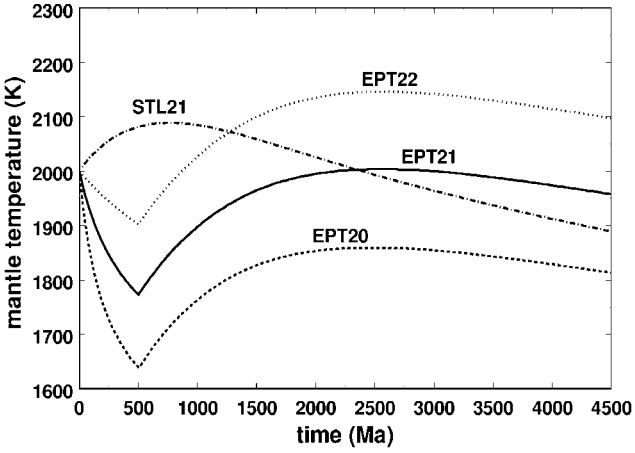

Figure 2. Mantle temperature as a function of time for three models with early plate tectonics. After 500 Ma plate tectonic ceases and stagnant lid convection sets in. Model EPT20 has a reference viscosity of 10^{20} Pas (dashed line), model EPT21 a reference viscosity of 10^{21} Pas (solid line) and model EPT22 a reference viscosity of 10^{22} Pas (dotted line). Also shown is the temperature for the stagnant lid convection model STL21 with a reference viscosity of 10^{21} Pas (dash-dotted line). This model assumes stagnant lid convection throughout the entire evolution of Mars.

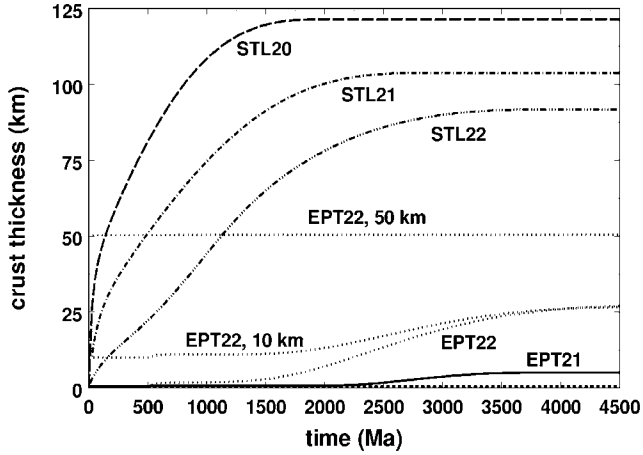

Figure 4. Crust thickness as a function of time for the early plate tectonics models EPT20 through EPT22 and the stagnant lid models STL20 through STL22. In addition, we show the crust thickness for a model (EPT22) with an assumed plate tectonics crust of 10 km and 50 km thickness.

[30] Both crust growth after the plate tectonics epoch and magnetic field generation during the plate tectonics epoch depend strongly on the cooling rate and on the mantle temperature attained at the end of this epoch. The smaller the mantle temperature then, the less crust will be produced thereafter. The larger the cooling rate, however, the more power is available to drive an early dynamo.

[31] The effects of the reference viscosity on post-plate tectonics crust growth are illustrated in Figures 4–6. These are the following:

[32] 1. For model EPT22 (reference viscosity 10^{22} Pas), crust is continuously generated (Figures 4 and 5) and grows to a present-day thickness of 27 km. At the onset of stagnant lid convection, the upper mantle temperature is still higher than the solidus and a partial melt zone (asthenosphere) is always present underneath the stagnant lid. The growth of the stagnant lid forces the asthenosphere to move to progressingly greater depth (Figure 6); the upper boundary of the asthenosphere sinks from about 100 km to 600 km depth. The initial decrease in the crust growth rate between 500 and 750 Ma and its later increase with a peak in the crust growth rate about 2000 Ma after the onset of stagnant lid convection reflects the evolution of the asthenosphere thickness. The latter, in turn, is a result of the competition between lid growth and sub-lid mantle warming.

[33] 2. For model EPT21 (reference viscosity 10^{21} Pas), crust growth starts late in this model and the crust grows to a total thickness of 5 km, a factor of 5 smaller than in model EPT22. Growth is restricted to the epoch between 1750 and 4300 Ma when an asthenosphere is present.

[34] 3. For model EPT20 (reference viscosity 10^{20} Pas), since there is no asthenosphere in this model, crust growth is absent during the stagnant lid regime. During plate

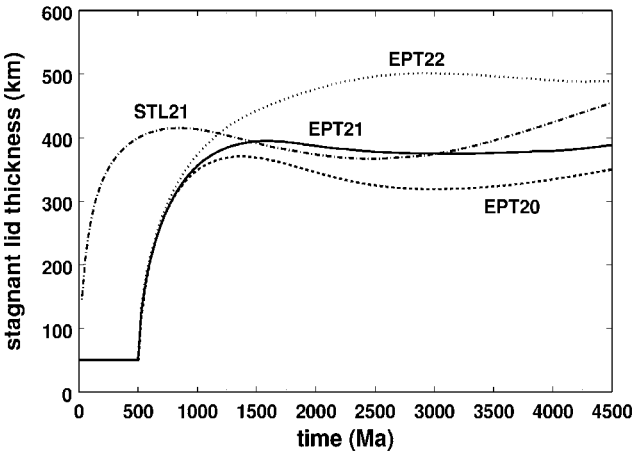

Figure 3. Stagnant lid thickness as a function of time. For further explanation see Figure 2.

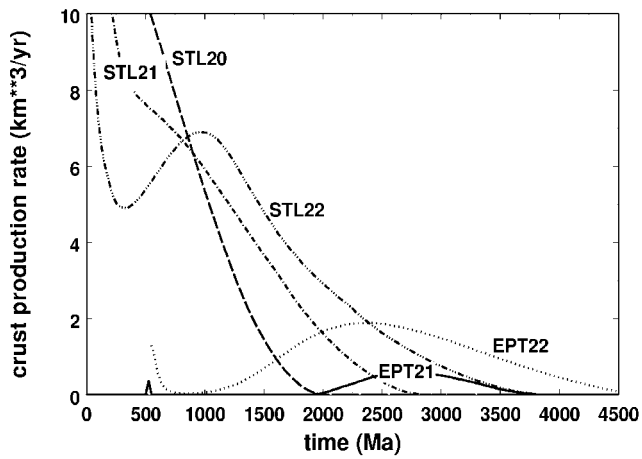

Figure 5. Crust production rate as a function of time for models EPT20 through EPT22 and STL20 through STL22.

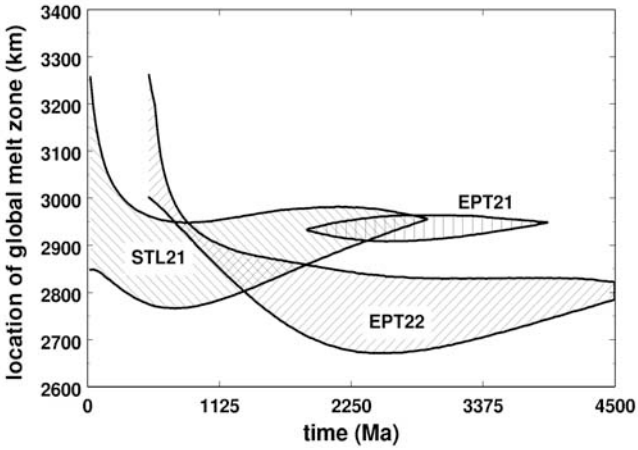

Figure 6. Location of the global melt zone as a function of time for model EPT21, EPT22 and STL21.

tectonics the planet's interior is cooled so efficiently that temperature will not rise above the solidus again. A crust in this model can thus only be produced during the phase of early plate tectonics.

[35] The effects of the reference viscosity on the heat flow from the core are shown in Figure 7. The core-mantle heat flow is always smaller than the critical heat flow for core convection in the post-plate tectonics era. There is also no inner core. Therefore a core dynamo is predicted to be absent during this period of time. For model EPT22 core convection is absent even during plate tectonics which precludes a Martian dynamo for this model altogether. For EPT21, the core-mantle heat flow is within the range of the critical heat flow, which makes an early dynamo possible. For EPT20, finally, the critical heat flow is clearly exceeded and an early dynamo is predicted.

3.2. Comparison With Stagnant Lid Models

[36] Figures 2 to 7 also show the results for models that have stagnant lid convection throughout the entire evolution. The reference viscosities for these models (STL20 to STL22) are 10^{20} to 10^{22} Pas and the models are equivalent to EPT20 to EPT22. The thermal evolutions differ significantly between these models, however. Starting with an initial mantle temperature of 2000 K (Figure 2), the temperature increases for STL21 at the time when the EPT models cool. A maximum temperature of about 2100 K is reached for STL21 after about 700 Ma. Thereafter, the temperature decreases steadily at a time when the EPT models heat up and the present-day temperature for STL21 is about 1900 K, roughly 50 K less than EPT21. The lid grows rapidly for STL21 as it does for EPT21, but 500 Ma earlier and after evolving in parallel for about 2 Ga, the STL21 lid reaches a 50 km greater thickness after 4.5 Ga (Figure 3). The crust production rates for STL20 and STL21 decrease steadily (Figure 5) and most of the crust is produced during the first few hundred million years. (It is interesting to note that STL22 has a secondary maximum in the crust growth rate at about 1000 Ma.) The present-day crust thickness in the STL models is between 90 and 120 km (Figure 4), an order of magnitude thicker than for the EPT models with the same parameter values. The thicker crust and the associated depletion of the mantle in heat sources is the reason why STL21 has a smaller present-day mantle temperature than EPT21. Even if we neglect the crust produced during the first 500 Ma, which is about 50 km for model STL21, crust formation is much more efficient in the subsequent evolution for the STL models as compared with the EPT models. The efficiency at crust formation in the EPT models increases with increasing reference viscosity. In the STL models, the efficiency at crust formation decreases with increasing reference viscosity although the mantle temperature and the degree of melting increase with increasing reference viscosity. The decrease of the crust formation rate here is caused by the decrease in convection speed with increasing reference viscosity. The crust formation rate depends on the convection speed through equation (1). In the EPT models crust formation is strongly affected by the heat transfer in the plate tectonics epoch. If the mantle cools comparatively slowly in the plate tectonics epoch, as it is the case for a higher reference viscosity, then more crust can be produced in the subsequent evolution due to higher mantle temperatures.

[37] Due to the slow cooling of the interior in the early evolution, the core-mantle heat flow remains smaller than the critical core heat flow for STL21 (and STL20 and STL22) during the whole evolution (Figure 7). This finding is consistent with the results of *Nimmo and Stevenson* [2000].

3.3. Effects of Crust Formation During the Plate Tectonics Epoch

[38] In this section, we demonstrate the effects of mantle depletion through plate tectonics crust formation on post-plate tectonics crust growth. We used model EPT22 and assumed initial crusts of 10 and 50 km thickness, respectively. These crusts are taken to be produced immediately at t = 0 and then the balance of crust formation and subduction is assumed to keep their thickness constant throughout the plate tectonics epoch. Their presumed basaltic composition is enriched in radioactive elements by a factor of 5 relative to the mantle and the mantle is taken to be depleted accordingly. For crust thicknesses of 10 and 50 km, the

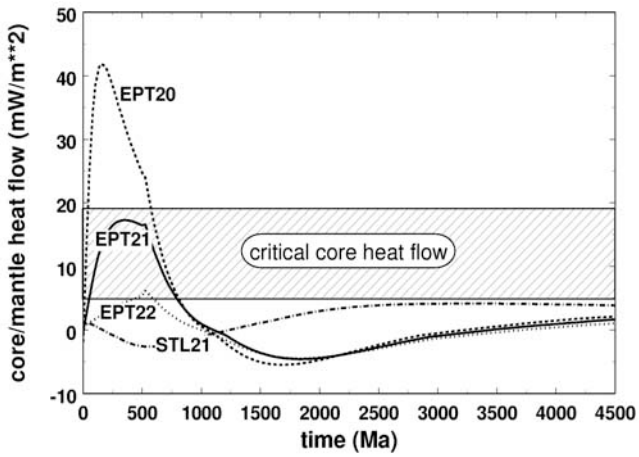

Figure 7. Core/mantle heat flow as a function of time for models EPT20 through EPT22 and STL21. The critical core heat flow, above which thermal core convection can set in, is indicated.

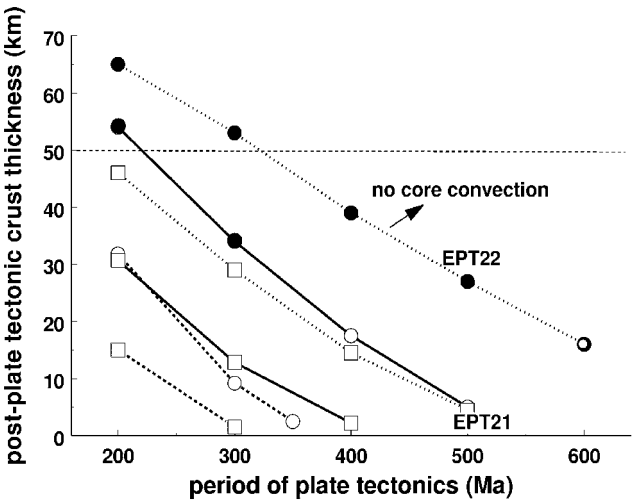

Figure 8. The post-plate tectonic crust thickness as a function of the length in time of the plate tectonics epoch is shown for models with a reference viscosity of 10^{20} Pas (dashed line), 10^{21} Pas (solid line) and 10^{22} Pas (dotted line). In addition, the temperature dependence of the mantle viscosity has been varied by varying the activation energy A. Models with A = 300 kJ/mole are marked with circles, models with A = 540 kJ/mole are marked with squares. (Models EPT21 and EPT22 with 500 Ma epochs of plate tectonics are marked for easier comparison). Models that have continuous crust production after the cessation of plate tectonics (such as EPT22, compare Figure 5) are indicated by solid circles or squares while those with a late (re-)onset of crust production (such as EPT21, Figure 5) are indicated by empty circles or squares. Shown is also the estimated minimum thickness of the crust of 50 km (dashed line) from *Zuber et al.* [2000]. The line for the models with A = 300 kJ/mole and $\eta_{ref} = 10^{22}$ Pas also marks the transition to a regime in which the heat flow from the core is subcritical. Models in the subcritical regime have either $\eta_{ref} > 10^{22}$ Pas or $A < 300$ kJ/mole.

mantle is depleted by about 5% and 25% of its initial inventory, respectively. As a consequence of the depletion of the mantle, post-plate tectonics heating in both models is weaker than in EPT22 and mantle melting is less (with a 10 km plate tectonics crust) or even absent (with a 50 km plate tectonics crust). In the 10 km model, 16 km of crust are produced in the post-plate tectonics epoch (Figure 4) to reach a total present-day thickness of 26 km, which is similar to the thickness obtained for EPT22. With a plate tectonics crust of 50 km thickness, no additional crust is produced. Thus the stronger the depletion of the mantle heat sources during plate tectonics, the less efficient is crust formation in the subsequent evolution with stagnant lid convection.

3.4. Length in Time of the Plate Tectonics Epoch

[39] The length in time of the plate tectonics epoch is another important parameter that determines the evolution of our Mars models. In Figure 8 the present-day crust thickness as a function of the length in time of the plate tectonics epoch is shown. In addition to varying the reference viscosity with values of 10^{20}, 10^{21} and 10^{22} Pas, we have varied the activation energy between 300 and 540 kJ mole^{-1}. For these models we again assume that no significant crust is produced during plate tectonics so that there is no early mantle depletion in radioactive elements. We mark models that show continuous post-plate tectonic crust growth with a solid symbol. Models that produce crust during a limited time only are marked with an empty symbol. In addition, we have indicated the minimum Martian crust thickness of 50 km estimated by *Zuber et al.* [2000] from gravity and topography data assuming Airy isostasy.

[40] In general, we find that the shorter the period of plate tectonics and the higher the reference viscosity, the more crust will be produced during the post-plate tectonics epoch. The final crust thickness is inversely proportional to the activation energy. The higher the activation energy, the more efficient is the cooling during the plate tectonics regime and the less crust is produced in the post-plate tectonics evolution. As the period of plate tectonics goes to zero, the crust thickness tends to that calculated for a stagnant lid model. For example, models with $\eta_{ref} = 10^{22}$ Pas and A = 300 kJ mole^{-1} tend toward STL22 under these conditions. The present-day crust thickness is smaller for most models than the minimum crust thickness estimated by *Zuber et al.* [2000].

[41] Models with $\eta_{ref} = 10^{22}$ Pas and an activation energy of 300 kJ mole^{-1} mark the transition to a regime in which the heat flow from the core is subcritical. Models in the subcritical regime have either bigger reference viscosities or smaller activation energies. Figure 8 clearly illustrates the dilemma of the early plate tectonics models: While these models can explain an early magnetic field they fail to produce a substantial post-plate tectonics crust.

4. Summary and Discussion

[42] We have investigated the consequences of a postulated early phase of plate tectonics on the formation of the Martian crust. Depending on the efficiency of early plate tectonics at cooling the mantle and core and depending on

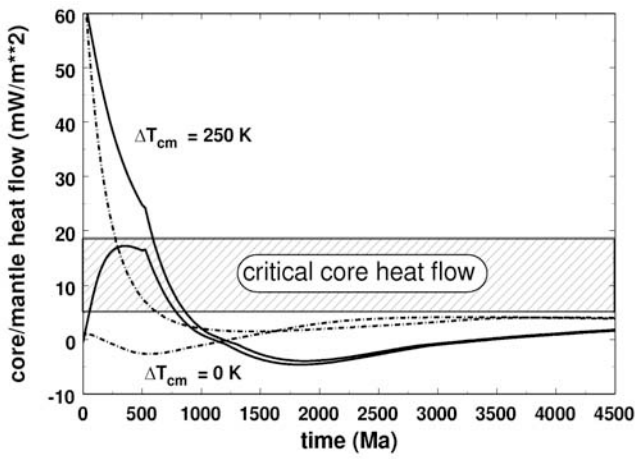

Figure 9. Core/mantle heat flow as a function of time for model EPT21 (solid line) and STL21 (dash-dotted line) with initial temperature differences across the core/mantle boundary of $\Delta T_{cm} = 0$ and $\Delta T_{cm} = 250$ K.

the heating of the interior in the subsequent evolution, there may be a continuous post-plate tectonic growth of the crust to a few tens of kilometres. A present-day crust of 50 km thickness and a significant crust production after the plate tectonics epoch is possible with a mantle rheology stiffer than that of the upper mantle of the present Earth ($\eta_{\mathrm{lref}} > 10^{22}$ Pas) and a length in time of the plate tectonics epoch of less than about 300 Ma. However, these models show a peak in the crust growth rate very late in the evolution, about 2000 to 2500 Ma ago. This is inconsistent with the observations, which suggest continuous declining of global volcanism since the Noachian with a possible secondary peak in the Early Hesperian before 3500 to 3800 Ma [e.g., *Head et al.*, 2001]. In addition, these models have a non-convecting core and therefore fail to produce an early magnetic field if the mantle and the core are in thermal equilibrium after core formation. Models in which plate tectonics cools the interior so efficiently that the core is convecting and a thermal dynamo can be driven have insignificant post-plate tectonics crust growth, some again with a late onset. The cooling efficiency depends on the chosen mantle viscosity, which we have varied over a broad range. The post-plate tectonics heating depends, in addition, on the Martian inventory of heat sources. We have adopted the widely accepted values for the primitive Martian mantle derived from the SNC meteorites but it is not likely that a variation of the heat source concentration in reasonable bounds will change our basic conclusion: Early plate tectonics models of Mars are difficult to reconcile with a substantial post-plate tectonics crust. The more efficient the cooling, and the more thermal power is available for the dynamo, the less likely is the production of crust after cessation of the plate tectonics regime.

[43] It may be argued that we have underestimated crust growth during the plate tectonics epoch. We have already argued further above that a plate tectonics crust can be marginally consitent with the estimated minimum value of the present-day crust. The production of more than a few tens of kilometres of crust during plate tectonics as we have shown in Figure 4 will frustrate crust production in the post-plate tectonics era. This leads to an approximate balance of plate tectonics crust and post-plate tectonics crust with a constant total thickness. For model EPT22, the most efficient crust producing EPT model, the post-plate tectonics crust thickness is about 25 km. Assuming a plate tectonics crust of more than this thickness, crust formation after plate tectonics is negligible. Interpretations of MOC data [*Head et al.*, 2001; *Frey et al.*, 2002] suggest considerable crust formation after the proposed end of the plate tectonics regime at about 4 Ga ago [e.g., *Connerney et al.*, 1999; *Nimmo and Stevenson*, 2000]. This is particularly true for the Northern Hemisphere where significant crust most likely in the Middle to Late Noachian [e.g., *Head et al.*, 2001] must have been formed after dynamo action, i.e., after plate tectonics, to explain the absence of prominent magnetic anomalies in the northern crustal province. Furthermore, in the Northern Hemisphere volcanic plains with an average thickness of 1 to 2 km were deposited in the Early Hesperian, which are possibly accompanied with intrusion rates resulting in an increase of the crust thickness between 10 and 20 km [*Greeley and Schneid*, 1991]. It should be noted, however, that the arguments against early plate tectonics would be weakened if it could be shown that the bulk of the crust was actually produced very early, e.g., in the Early Noachian.

[44] Other parameters such as the initial mantle temperature and the solidus temperature of the mantle rock have been tested in additional calculations for their influence on the results. Varying the initial temperature has little effect. During the first few hundred million years the mantle temperature adjusts almost to the same value independent of the starting value. A higher crust production rate and a thicker present-day crust thickness can be obtained by lowering the melting temperature. We have used the solidus and liquidus of dry peridotite [*Takahashi*, 1990], which represents reasonably well the solidus and liquidus of the assumed Martian mantle composition [*Bertka and Holloway*, 1994; *Schmerr et al.*, 2001]. Assuming a 100 K lower melting temperature, for instance due to the presence of water in the mantle, a 20 km thicker present-day crust thickness is obtained. However, the presence of fluid phases (water and/or melt) also implies a lower viscosity of the mantle [e.g., *Karato and Wu*, 1993; *Kohlstedt and Zimmermann*, 1996], which results again, due to faster cooling in the plate tectonics regime, in a smaller crust growth rate thereafter. In addition, the chemistry of the SNC meteorites has been interpreted to suggest that the Martian mantle stayed dry since the time of core formation [*Dreibus and Wänke*, 1985, 1987; *Carr and Wänke*, 1992], although new geochemical evidence for magmatic water within Mars raises some doubts [*McSween et al.*, 2001]. Water added during homogeneous accretion may have reacted with metallic iron. The water that was apparently on the surface must have been added late during accretion and must have stayed on the surface. The dryness of the Martian mantle as well as the W isotope characteristics in the SNC meteorites has been used to argue against plate tectonics on Mars [e.g., *Halliday et al.*, 2001].

[45] Crust production may have been increased by local plume volcanism. Mantle plumes may transport hot mantle rock from the core-mantle boundary to the surface. Eventually the plume may pass the solidus and melt may be generated underneath the lithosphere. In the present model, the contribution of plume volcanism is not separated from the global crust production because we compare the average mantle temperature with the solidus. It may be argued that we strongly underestimated the crust production rate at times when there is no global asthenosphere. In the presence of strong lateral temperature variations in the mantle with hot upwellings and cold downwellings, the average mantle temperature can be below the solidus but melt can be locally generated in the hot upwellings. For the generation of plume volcanism, however, a thermal boundary layer at the base of the mantle is required to initiate plumes by thermal instabilities. A thermal boundary layer at the bottom of the mantle requires sufficient heat flow from the core. If the mantle is mainly heated from within, plumes are very weak and the associated volcanism is insignificant or even not present. In that case mantle convection is dominated by cold downwellings and the upwelling flow is broad with a small temperature contrast relative to the average mantle. With the present simple parameterized model we cannot resolve the convection structure. However, as Figure 7 shows, the heat flow from the core in the EPT models in the post-plate

tectonics epoch is mostly negative meaning that heat is flowing from the mantle to the core rather than from the core to the mantle, to compensate for the core cooling in the plate tectonics epoch. Convection models show that plumes cannot develop under these conditions. Even when the heat flow out of the core becomes slightly positive after about 3 Ga, the temperature difference across the core-mantle boundary layer remains smaller than 50 K under which conditions the formation of a plume is still questionable. Even if a weak plume formed, its excess temperature at the core/mantle boundary would be less than 50 K. The excess temperature decreases with height above the core/mantle boundary because of adiabatic cooling and heat diffusion [e.g., *Albers and Christensen*, 1996] and is less than a few tens K beneath the lithosphere. This conclusion is largely independent of any assumed mantle depletion due to plate tectonics crust formation. Therefore we argue that plume volcanism cannot be used to explain post-plate tectonics crust formation at a significant level.

[46] It is likely that the crust thicknesses presented in this paper are actually overestimated rather than underestimated. We assumed that all melt could freely rise to the surface to produce new crust. The asthenosphere, however, is at a depth of 400 to 700 km. Melt can only rise toward the surface if the lithosphere above is sufficiently permeable. This permeability is likely due to cracks in the crust and lithosphere [e.g., *Spera*, 1980]. The permeability is expected to decrease with depth as cracks are expected to close in response to the increasing pressure. Therefore it is likely that significant parts of the rising melt will never make it to the surface or to the crust. Moreover, the compressibility of magma is higher than the compressibility of rock such that beyond a critical depth, the magma will have a higher density than the surrounding mantle rock. The magma under these circumstances will have neutral or even negative buoyancy and will not rise but may even tend to sink. Sink-float tests of olivine in a melt of a model Martian mantle composition suggest that melt deeper than about 7.4 GPa (in approximately 600 km depth of the Martian mantle) may not be able to rise to the surface [*Ohtani et al.*, 1998].

[47] In summary, the calculated present-day crust thicknesses for the presented models are upper bounds. Although we cannot exclude the possibility of an early phase of plate tectonics, the results show that it is much easier to explain the observations of a monotonically declining crust production rate through the Noachian and Hesperian and a present-day crust thickness of more than about 50 km with Mars being in the stagnant lid regime throughout the entire evolution. Further arguments against early plate tectonics arise from cosmochemical data. Cosmochemical data require early mantle differentiation to explain the ^{182}Hf-^{182}W [*Lee and Halliday*, 1997; *Halliday et al.*, 2001] and other isotope data [e.g., *Shih et al.*, 1982; *Chen and Wasserburg*, 1986; *Jagoutz*, 1991; *Borg et al.*, 1997] of the SNC-meteorites. The data suggest also that there are chemical heterogeneities in the Martian mantle that should have been produced in the first 20 Ma of its evolution by silicate melting and core differentiation and which are preserved for most of the Martian history. The existence of those early and long-lasting heterogeneities is difficult to explain with early plate tectonics. In the case of stagnant lid convection the geochemical heterogeneity may persist in the non-convecting part of the upper mantle, which forms rapidly (Figure 3) and stay separate during the entire evolution.

[48] It may be argued that due to the high mantle temperatures in the stagnant lid regime crust formation is too efficient and that the calculated present-day crust thicknesses of the STL models are unrealistic. The growth history of the crust, however, is strongly dependent on the initial temperature distribution, the redistribution of radioactive elements due to crust growth, the permeability of the growing lithosphere for mantle derived melt, and on the mantle rheology. Depending on the choice of parameter values, a present-day crust thickness between a few kilometers and more than 100 km is possible for Mars in the STL models. A more detailed discussion of STL models is beyond the scope of the present paper as we mainly focus on the general difference between the two evolution models. Results describing the various effects on crust production in the stagnant lid regime have been described in a paper by *Hauck and Phillips* [2002].

[49] One main argument for an early period of plate tectonics by *Nimmo and Stevenson* [2000] is that the efficient heat transfer mechanism due to plate tectonics will drive convection in the core and thus effectively power magnetic field generation. More recently, *Stevenson* [2000] argued for core superheat to allow molten iron-rich cores after core formation. In Figure 9 we compare models EPT21 and STL21 with $\Delta T_{cm} = 0$ and $\Delta T_{cm} = 250$ K. The difference between the two models with initially superheated cores with respect to core convection lies mostly with the time of duration of core convection, which is a factor of two longer for the early plate tectonics model. Judging from the present results, the presently favored models of the magnetic and crustal evolution of Mars (magnetic field generation in the Early Noachian and crust formation throughout the Noachian and Early Hesperian) are most easily reconciled in a uniformitarian model in which Mars has been in the one-plate, stagnant lid regime throughout its history.

[50] **Acknowledgments.** We have profited from discussions with Gerald Schubert and from constructive reviews by Olivier Forni and an anonymous reviewer.

References

Acuña, M. H., et al., Global distribution of crustal magnetism discovered by the Mars Global Surveyor MAG/ER Experiment, *Science*, *284*, 790–793, 1999.

Albers, M., and U. R. Christensen, The excess temperature of plumes rising from the core-mantle boundary, *Geophys. Res. Lett.*, *23*, 3567–3570, 1996.

Bandfield, J. L., V. E. Hamilton, and P. R. Christensen, A global view of Martian surface composition from MGS-TES, *Science*, *281*, 1626–1630, 2000.

Basaltic Volcanism Study Project (BVSP), *Basaltic Volcanism on the Terrestrial Planets*, 1286 pp., Pergamon, New York, 1981.

Bertka, C. M., and J. R. Holloway, Anhydrous partial melting of an iron-rich mantle, I, Subsolidus phase assemblages and partial melting phase relations at 10 to 30 kbar, *Contrib. Mineral. Petrol.*, *115*, 313–322, 1994.

Borg, L. E., L. E. Nyquist, L. A. Taylor, H. Wiesmann, and C.-Y. Shih, Constraints on Martian differentiation processes from Rb-Sr and Sm-Nd isotopic analyses of the basaltic shergottite QUE94201, *Geochim. Cosmochim. Acta*, *22*, 4915–4931, 1997.

Breuer, D., and T. Spohn, Possible flush instability in mantle convection at the Archean-Proterozoic transition, *Nature*, *378*, 608–610, 1995.

Breuer, D., T. Spohn, and U. Wüllner, Mantle differentiation and the crustal dichotomy of Mars, *Planet. Space. Sci.*, *41*, 269–283, 1993.

Carr, M. H., and H. Wänke, Earth and Mars: Water inventories as clues to accretional histories, *Icarus*, *98*, 61–71, 1992.

Chen, J. H., and G. J. Wasserburg, Formation ages and evolution of Shergotty and its parent planet from U-Th-Pb systematics, *Geochim. Cosmochim. Acta*, *50*, 955–968, 1986.
Choblet, G., and C. Sotin, 3D thermal convection with variable viscosity: Can transient cooling be described by a quasi-static scaling law?, *Phys. Earth Planet. Inter.*, *119*, 321–336, 2000.
Choblet, G., and C. Sotin, Early transient cooling of Mars, *Geophys. Res. Lett.*, *28*, 3035–3038, 2001.
Condie, K. C., *Plate Tectonics and Crustal Evolution*, 4th ed., 282 pp., Butterworth-Heinemann, Woburn, Mass., 1997.
Connerney, J. E. P., M. H. Acuña, P. Wasilewski, N. F. Ness, H. Rème, C. Mazelle, D. Vignes, R. P. Lin, D. Mitchell, and P. Cloutier, Magnetic lineations in the ancient crust of Mars, *Science*, *284*, 794–798, 1999.
Davaille, A., and C. Jaupart, Transient high-Rayleigh-number thermal convection with large viscosity variations, *J. Fluid Mech.*, *253*, 141–166, 1993.
Davies, G. F., Plates, plumes, and mantle convection, in *The Earth's Mantle: Composition, Structure, and evolution*, edited by I. Jackson, pp. 228–258, Cambridge Univ. Press, New York, 1998.
Dreibus, G., and H. Wänke, Mars: A volatile rich planet, *Meteoritics*, *20*, 367–382, 1985.
Dreibus, G., and H. Wänke, Volatiles on Earth and Mars: A comparison, *Icarus*, *71*, 225–240, 1987.
Frey, H. V., J. H. Roark, K. M. Shockey, E. L. Frey, and S. E. H. Sakimoto, Ancient lowlands on Mars, *Geophys. Res. Lett.*, *29*(10), 1384, doi:10.1029/2001GL013832, 2002.
Grasset, O., and E. M. Parmentier, Thermal convection in a volumetrically heated, infinite Prandtl number fluid with strongly temperature-dependent viscosity: Implications for planetary thermal evolution, *J. Geophys. Res.*, *103*, 18,171–18,181, 1998.
Greeley, R., and B. D. Schneid, Magma generation on Mars: Amounts/rates, and comparisons with Earth, Moon and Venus, *Science*, *254*, 996–998, 1991.
Gurnis, M., and G. F. Davies, Simple parametric models of crustal growth, *J. Geodyn.*, *3*, 105–135, 1985.
Halliday, A. N., H. Wänke, J.-L. Birck, and R. N. Clayton, The accretion, composition and early differentiation of Mars, *Space Sci. Rev.*, *96*, 197–230, 2001.
Hartmann, W. K., and G. Neukum, Cratering chronology and the evolution of Mars, *Space Sci. Rev.*, *96*, 165–194, 2001.
Hartmann, W. K., M. Malin, A. McEwen, M. Carr, L. Soderblom, P. Thomas, E. Danielson, P. James, and J. Veverka, Recent volcanism on Mars from crater counts, *Nature*, *397*, 586–589, 1999.
Hauck, S. A., II, and R. J. Phillips, Thermal and crustal evolution of Mars, *J. Geophys. Res.*, *107*(E7), 5052, doi:10.1029/2001JE001801, 2002.
Head, J. W., R. Greeley, M. P. Golombek, W. K. Hartmann, E. Hauber, R. Jaumann, P. Masson, G. Neukum, L. E. Nyquist, and M. H. Carr, Geological processes and evolution, *Space Sci. Rev.*, *96*, 263–292, 2001.
Head, J. W., III, M. A. Kreslavsky, and S. Pratt, Northern lowlands of Mars: Evidence for widespread volcanic flooding and tectonic deformation in the Hesperian Period, *J. Geophys. Res.*, *107*(E1), 5003, doi:10.1029/2000JE001445, 2002.
Jagoutz, E., Chronology of SNC meteorites, *Space Sci. Rev.*, *56*, 13–22, 1991.
Karato, S., and P. Wu, Rheology of the upper mantle: A synthesis, *Science*, *260*, 771–778, 1993.
Kohlstedt, D. L., and M. E. Zimmerman, Rheology of partially molten mantle rocks, *Annu. Rev. Earth Planet. Sci.*, *24*, 41–62, 1996.
Lee, D.-C., and A. N. Halliday, Core formation on Mars and differentiated asteroids, *Nature*, *388*, 854–857, 1997.
McEwen, A. S., M. C. Malin, M. H. Carr, and W. K. Hartmann, Voluminous volcanism on Early Mars revealed in Valles Marineris, *Nature*, *397*, 584–586, 1999.
McKenzie, D. P., and M. J. Bickle, The volume and composition of melt generated by extension of the lithosphere, *J. Petrol.*, *29*, 625–679, 1988.
McSween, H. Y., T. L. Grove, R. C. F. Lentz, J. C. Dann, A. H. Holzheid, L. R. Riciputi, and J. G. Ryan, Geochemical evidence for magmatic water within Mars from pyroxenes in Shergotty meteorite, *Nature*, *409*, 487–490, 2001.
Nimmo, F., and D. Stevenson, Influence of early plate tectonics on the thermal evolution and magnetic field of Mars, *J. Geophys. Res.*, *105*, 11,969–11,979, 2000.
Norman, M. D., Thickness and composition of the Martian crust revisited: Implications of an ultradepleted mantle with a Nd isotopic composition like that of QUE94201, (abstract), *Lunar Planet. Sci.*, *XXXIII*, 1157, 2002.
Ohtani, E., A. Suzuki, and T. Kato, Flotation of olivine and diamond in mantle melt at high pressure: Implications for fractionation in the deep mantle and ultradeep origin of diamond, in *Properties of Earth and Planetary Materials at High Pressure and Temperature*, *Geophys. Monogr. Ser.*, vol. 101, edited by M. H. Manghnani and T. Yagi, pp. 227–239, AGU, Washington, D. C., 1998.
Oxburgh, E. R., and E. M. Parmentier, Compositional and density stratification in oceanic lithosphere-causes and consequences, *J. Geol. Soc. London*, *90*, 678–684, 1977.
Peltier, W. R., Mantle viscosity and ice-age ice sheet topography, *Science*, *273*, 1359–1364, 1996.
Reymer, A. P. S., and G. Schubert, Phanerozoic and Precambrian crustal growth, in *Proterozoic Lithospheric Evolution*, *Geodyn. Ser.*, vol. 17, edited by A. Kröner, pp. 1–9, AGU, Washington, D. C., 1987.
Richter, F. M., Experiments on the stability of convection rolls in fluids whose viscosity depends on temperature, *J. Fluid Mech.*, *89*, 553–560, 1978.
Schmerr, N. C., Y. Fei, and C. M. Bertka, Extending the solidus for a model iron-rich Martian mantle composition to 25 GPa (abstract), *Lunar Planet. Sci.*, *XXXII*, 1157, 2001.
Schubert, G., and T. Spohn, Thermal history of Mars and the sulfur content of its core, *J. Geophys. Res.*, *95*, 14,095–14,104, 1990.
Schubert, G., P. Cassen, and R. E. Young, Subsolidus convective cooling histories of terrestrial planets, *Icarus*, *38*, 192–211, 1979.
Schubert, G., S. C. Solomon, D. L. Turcotte, M. J. Drake, and N. H. Sleep, Origin and thermal evolution of Mars, in *Mars*, edited by H. H. Kieffer et al., pp. 147–183, Univ. of Ariz. Press, Tucson, 1992.
Schubert, G., C. T. Russell, and W. B. Moore, Timing of the Martian dynamo, *Nature*, *408*, 666–667, 2000.
Schubert, G., D. L. Turcotte, and P. Olson, *Mantle Convection in the Earth and Planets*, 940 pp., Cambridge Univ. Press, New York, 2001.
Shih, C.-Y., L. E. Nyquist, D. D. Bogard, G. A. Mckay, J. L. Wooden, B. M. Bansal, and H. Wiesman, Chronology and petrogenesis of young achondrites, Shergotty, Zagami and ALHA77005: Late magmatism on a geologically active planet, *Geochim. Cosmochim. Acta*, *46*, 2323–2344, 1982.
Sleep, N. H., Martian plate tectonics, *J. Geophys. Res.*, *99*, 5639–5655, 1994.
Sohl, F., and T. Spohn, The structure of Mars: Implications from SNC-meteorites, *J. Geophys. Res.*, *102*, 1613–1635, 1997.
Solomatov, V. S., Scaling of temperature- and stress-dependent viscosity, *Phys. Fluids*, *7*, 266–274, 1995.
Spera, F. J., Aspects of magma transport, in *Physics of Magma Transport*, edited by R. B. Hargraves, pp. 265–323, Princeton Univ. Press, Princeton, N. J., 1980.
Spohn, T., Mantle differentiation and thermal evolution of Mars, Mercury, and Venus, *Icarus*, *90*, 222–236, 1991.
Spohn, T., and D. Breuer, Mantle differentiation through continental crust growth and recycling and the thermal evolution of the Earth, in *Evolution of the Earth and Planets*, *Geophys. Monogr. Ser.*, vol. 74, edited by E. Takahashi, R. Jeanloz, and D. C. Rubie, pp. 55–71, AGU, Washington, D. C., 1993.
Spohn, T., and G. Schubert, Modes of mantle convection and the removal of heat from the Earth interior, *J. Geophys. Res.*, *87*, 4682–4696, 1982.
Stevenson, D. J., Core superheat, *Eos Trans. AGU*, *81* (48), Fall Meet. Suppl., abstract T11F-08, 2000.
Stevenson, D. J., Mars core and magnetism, *Nature*, *412*, 214–219, 2001.
Stevenson, D. J., T. Spohn, and G. Schubert, Magnetism and thermal evolution of the terrestrial planets, *Icarus*, *54*, 466–489, 1983.
Takahashi, E., Speculations on the archean mantle: Missing link between komatiite and depleted garnet peridotite, *J. Geophys. Res.*, *95*, 15,941–15,954, 1990.
Treiman, A. H., M. J. Drake, M. J. Janssens, R. Wold, and M. Ebihara, Core formation in the Earth and shergottite parent body (SPB): Chemical evidence from basalts, *Geochim. Cosmochim. Acta*, *50*, 1071–1091, 1986.
Turcotte, D. L., and J. Huang, Implications on crust formation on Mars from parameterized convection calculations, *Proc. Lunar Planet. Sci. Conf. 21st*, abstract 1266, 1990.
Turcotte, D. L., and G. Schubert, *Geodynamics*, John Wiley, New York, 1982.
Turcotte, D. L., B. D. Malamud, and R. Shcherbakov, Analyses of Mars topography, gravity and aeroid: Implications for Tharsis and Hellas, *Geophys. Res. Abstr.* [CD-ROM], *3*, 7241, 2001.
Weizman, A., D. J. Stevenson, D. Prialnik, and M. Podolak, Modeling the volcanism on Mars, *Icarus*, *150*, 195–205, 2001.
Zuber, M. T., The crust and mantle of Mars, *Nature*, *412*, 220–227, 2001.
Zuber, M. T., et al., Internal structure and early thermal evolution of Mars from Mars Global Surveyor topography and gravity, *Science*, *287*, 1788–1793, 2000.

D. Breuer and T. Spohn, Institut für Planetologie, Universität Münster, Wilhelm Klemm Strasse 10, D-48149, Münster, Germany. (breuer@uni-muenster.de)